SYNCHROTRON INFRARED MICROSPECTROSCOPY STUDY OF THE ORIENTATION OF AN ORGANIC SURFACTANT ON A MICROSCOPICALLY ROUGH STEEL SURFACE

Kateřina Lepková, Wilhelm van Bronswijk, Vedapriya Pandarinathan, Rolf Gubner

Corrosion Centre for Education, Research and Technology
Department of Chemistry, Curtin University
Perth, WA 6845, Australia

Corresponding author:

Kateřina Lepková

Department of Chemistry, Curtin University,
G.P.O. Box U1987, Perth, WA 6845, Australia
E-mail: k.lepkova@curtin.edu.au
Telephone: +61892667319
Fax: +61892662300

ABSTRACT

The performance of organic surfactants as corrosion inhibitors is influenced by the mechanism of adsorption and the resulting molecular orientation on the substrate. The molecular orientation of 1-dodecylpyridinium chloride (DPC) deposited on non-corroded 1030 mild steel and after corrosion in a carbon dioxide environment has been investigated using synchrotron infrared microspectroscopy. DPC mitigates the corrosion process by adsorbing at the steel surface and forming a protective layer.

Infrared spectra analogous to polarized grazing angle spectra were obtained from a microscopically rough surface using a synchrotron source. The appearance of negative and positive absorption bands in the spectra, when using synchrotron radiation, is discussed in terms of the optical system used. The presence of the DPC surfactant at the steel surface is shown by the CH_2 and CH_3 infrared absorption bands of the aliphatic chain of the DPC molecule. The infrared spectra provide direct evidence on the orientation of DPC at the steel substrate. The aliphatic chain of the surfactant is tilted orthogonally, but not perpendicular to the substrate plane. The absence of significant absorption bands characteristic of the pyridinium ring of DPC indicates its orientation parallel to the substrate plane, and an adsorption mechanism involving π-bonding with the steel.

This study demonstrates the applicability of synchrotron infrared microspectroscopy to the investigations of thin organic films on microscopically rough steel surfaces, and can facilitate further investigations of thin films on metallic surfaces and monolayer studies in general.

KEYWORDS

Infrared microspectroscopy; Synchrotron; Steel; Molecular orientation; Organic surfactant; Corrosion.

1. INTRODUCTION

Organic surfactants which adsorb on a variety of substrates have been used in numerous applications, such as ore flotation, stabilization of foams and emulsions, wetting control and corrosion inhibition [1,2]. In corrosion inhibition, organic surfactants are used to mitigate corrosion reactions by adsorbing on the metallic substrates and forming a protective layer. The performance of organic surfactants as corrosion inhibitors depends on their bonding and molecular orientation towards the substrate. It has been suggested, for example, that chemisorbed organic surfactants are more persistent than physisorbed organic surfactants, and are therefore preferred as batch-treatment corrosion inhibitors [3].

Reflection-absorption infrared spectroscopy is a suitable technique for determining the molecular orientation of organic compounds on metallic substrates. Previous studies have established that at high angles of incidence thin surface layers exhibit high absorption of infrared radiation that is polarized perpendicular to the reflection plane (metallic substrate). In this arrangement, with application of the metal surface selection rule, only molecular vibrations perpendicular to the reflection plane absorb the infrared light and thus appear in the spectra. Since the recorded absorption bands are related to the different parts of the organic compound, the molecular orientation at the surface can be determined [4-6].

Detailed information on the nature of the surface layers is required in order to elucidate the exact mechanisms of the corrosion inhibition. However, when examining organic layers at corroded metallic substrates, determining the absorption of infrared radiation is often complicated due to the topography of the corrosion-roughened surface, and the limited thickness and heterogeneity of the surface layer.

To test the applicability of synchrotron-sourced infrared microspectroscopy to analyse such complex surfaces, we have studied a carbon steel surface that had been immersed in a 1-dodecylpyridinium chloride (DPC) solutions in nitrogen or carbon dioxide saturated media. Many oil and gas systems operate in carbon dioxide environments where corrosion is caused by carbonic acid. Pyridinium-based surfactant molecules with a long alkyl chain, such as DPC, are used as oil-well corrosion inhibitors [3], and pyridinium compounds efficiently inhibit corrosion reactions at iron surfaces in acidic media [7]. It has been proposed that DPC adsorbs at a metal surface through the aromatic ring, with the hydrophobic aliphatic chain oriented into the solution [3,8]. However, no direct evidence of the molecular orientation of DPC has been presented and the exact mechanism of the DPC adsorption is unknown.

A complementary method for studying the orientation and absorption mechanism of pyridine and pyridinium compounds on surfaces is surface enhanced Raman spectroscopy (SERS). SERS studies of pyridine/pyridinium adsorption at non-modified steel surfaces (iron-carbon alloys with original crystalline structure) have not been performed as the modification of the substrate (surface roughness) is required for quality SER spectra. Furthermore, the SERS technique is not sensitive to π-bonded organic compounds and can only detect pyridinium compounds that are bonded to the substrate through the nitrogen atom [9]. Hence, infrared spectroscopy can provide additional information on the surface orientation of the organic compounds. From SERS data of pyridine and pyridinium compounds adsorbed on iron-deposited silver substrates two different adsorption mechanisms were proposed: (1) coordination bonding between the nitrogen atom of the aromatic ring and the metal (σ-bond) resulting in non-parallel orientation of the aromatic ring at the substrate [10,11], and (2) π-electron interaction between the aromatic ring and the metallic substrate, which results in parallel orientation of the aromatic ring at the substrate. The π-

electrostatic interaction can be influenced by the presence of halide ions that pre-adsorb at the surface [10-12]. It has also been proposed that an individual compound can adsorb through both of the mechanisms, depending on the nature of the substrate and the composition of the corrosive solution [12].

In this study, we use a strongly polarized synchrotron source infrared beam and a Cassegrain objective to record infrared spectra without a polariser in the beam that are equivalent to those obtainable from flat metallic and non-conductor surfaces when a polariser is used. The data allow the surface orientation of the organic surfactant to be determined. If the pyridinium ring and aliphatic chain of the DPC molecule are oriented non-parallel with respect to the steel surface then both parts of the molecule would interact with infrared radiation. This would be indicative of the σ-bonding of the pyridinium ring at the substrate through the nitrogen atom. On the other hand, parallel orientation of the pyridinium ring to the steel surface would not result in its interaction with infrared radiation. Therefore, the absence of the in-plane ring absorption bands in the infrared spectra would be indicative of π-bonding of the pyridinium ring at the substrate.

2. MATERIALS AND METHODS

2.1 Materials

The carbon steel studied had the following elemental composition (wt. %): C 0.37, Mn 0.80, Si 0.28, Cr 0.09, P 0.01, Ni 0.01, Fe balance. Steel samples (20 mm diameter) were ground with SiC paper to 1200 grit and then polished to a surface finish of 1 µm using diamond suspensions. This polishing method consistently results in carbon steel surfaces with average surface roughness (root mean square, Rq) of ~ 0.4 µm, confirmed with visible light microscopy using an

Alicona Infinite Focus (Alicona Imaging GmbH, Austria). The polished samples were cleaned with methanol and ultra-pure deionised water and dried with nitrogen prior to immersion in the test solution. The samples were dried with nitrogen after the test and stored under vacuum until further analysis. Care was taken when handling the samples to minimize their exposure to air.

The testing solutions were (1) 500 ppm of 1-dodecylpyridinium chloride hydrate ($C_{17}H_{30}ClN.xH_2O$; Sigma-Aldrich, 98%) in deionised ultra-pure water saturated with nitrogen; and (2) 500 ppm of 1-dodecylpyridinium chloride hydrate ($C_{17}H_{30}ClN.xH_2O$; Sigma-Aldrich, 98%) in brine, consisting of 0.5 M sodium chloride (NaCl; Ajax Finechem, 99.9%) and $1x10^{-3}$ M sodium hydrogen carbonate ($NaHCO_3$; Merck, 99.5%), saturated with high-purity carbon dioxide (99.99%) before and during the experiments. The chemical structure of the DPC molecule is given in Fig. 1.

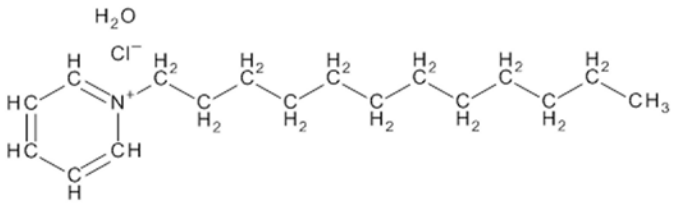

Fig. 1. Chemical structure of 1-dodecylpyridinium chloride hydrate.

Two types of samples are used in this study and differ by the degree of corrosion. The non-corroded samples were prepared by immersion into solution (1) at ambient temperature (20 °C) for 20 min. These conditions were expected to have little effect on the surface properties of the steel, such as roughness and reflectivity. Therefore these samples are referred to as non-corroded for the purpose of this study. The corroded samples were prepared in solution (2) at 60 °C for 24 h, i.e. the corrosion took place in the presence of the inhibitor, as it would in its industrial environment.

The DPC-treated steel samples and untreated (plain) steel, used for a background measurement, were placed into an enclosed compartment surrounding the infrared microscope assembly, which was continuously purged with dry nitrogen. After positioning the sample, the atmosphere inside the compartment was left to stabilize for 30 min. before the infrared analysis. This procedure minimized the amount of water vapour and carbon dioxide appearing in the recorded spectra.

The infrared spectrum of the DPC powder was recorded using Attenuated Total Reflectance and a Perkin-Elmer Spectrum 100 spectrometer. The DPC powder was used as received.

The corroded samples were also analyzed with a Hyperion 3000 microscope with a Focal Plane Array (FPA) detector and conventional infrared source. The aperture size was 100 x 100 μm. The untreated (plain) steel was used as a background for the FPA analysis.

2.2 Atomic force microscopy (AFM) measurement and analysis

In-situ AFM analysis was carried out using an Agilent Picoplus AFM Multimode apparatus in a soft contact mode. A silicon nitride cantilever (type DNP) with a spring constant of 0.32 Nm^{-1} was used. The samples were mounted on the AFM liquid cell holder and the test solution (1) was continuously recirculated through the cell during the experiment.

2.3 Surface coverage measurement

The coverage of the corroded steel surface with DPC was determined from corrosion rates obtained from linear polarization resistance (LPR) analysis. A standard three-electrode system and solution (2) with and without DPC were used, and the steel samples were polarized in the potential range of ± 10 mV vs. open circuit potential in a sweep rate of 0.6 V h^{-1} using a Gill

Potentiostat (ACM Instruments, UK). The corrosion rates from the LPR measurements were calculated according to the standard procedure given elsewhere [13].

2.4 Corroded steel roughness measurement

The roughness of the corroded steel surfaces was measured using an Alicona InfiniteFocus visible light microscope (Alicona Imaging GmbH, Austria) with 50x magnification objective. A surface roughness parameter R_q (root mean square) was calculated from the surface heights using the Alicona IFM 3.5 software. The samples were briefly exposed to air during the surface roughness measurements, which followed the infrared spectroscopy analysis.

2.5 Synchrotron infrared spectral measurement and analysis

Infrared spectroscopy was performed on the infrared microspectroscopy beamline at the Australian Synchrotron using a Brüker Hyperion 2000 microscope coupled to a Vertex V80v FTIR spectrometer. A Cassegrain objective with 36x magnification was used and the aperture of the microscope was set at 20 x 20 μm. Spectra acquisition and processing was performed using Opus 6.5 software (Brüker optics).

The FTIR spectra were recorded in reflectance mode with a resolution of 4 cm^{-1}, using a liquid nitrogen-cooled MCT detector. For each spectrum, 256 scans were collected in the range of 3800-800 cm^{-1}. A total of 256 background scans were collected on untreated (plain) steel of the same elemental composition as the test samples. 256 scans were also collected using a gold mirror to obtain an absorbance spectrum of the untreated steel. The untreated steel and gold mirror were placed in the nitrogen-purged compartment at the same time as the test samples to ensure identical environmental conditions for collection of the background and the sample spectra. The spectra are presented in terms of $-log\ (I/I_0)$, where I and I_0 are the absorption

intensities in the single channel spectra obtained from the test sample and the untreated steel, respectively.

2.5.1 Optical parameters

The Australian Synchrotron IR microscope beamline uses only the bending magnet radiation. The polarization ellipse of this radiation is not significantly affected by the optical path of the microscope [14]. Infrared spectra were acquired with a predominantly *p*-polarized synchrotron beam (parallel (*p*): perpendicular (*s*) ~ 4:1), but without a polarizer in the beam. A reverse Cassegrain objective was used and hence the polarized synchrotron infrared beam's incidence angle approaching the surface changes within the hollow cone, which is approximately 30^{o}, i.e. the incident beam will have both a *p* and an *s* component relative to the microscope plane. Infrared spectroscopy with a synchrotron source applied in polarization studies, particularly in transmission mode showed that orientation information could be obtained with the use of the intrinsic synchrotron source and without a polarizer [15,16].

At optically flat metallic surfaces that are reflective (conductors), *p*-polarization has non-zero strength and interacts with vibrations perpendicular to and at the surface, whereas *s*-polarization has zero field strength and does not interact. The intensity of the absorption bands from thin surface films at metallic substrates increases with increasing angle of incidence, with maximum absorbance obtained at a grazing angle of 88^{o} [17]. At low angles of incidence, such as used in this work, the surface enhancement of the adsorbed molecules on the steel surface is not achieved however absorption bands with lower intensity to those recorded at the optimum grazing angles can be observed [17,18]. The position and shape of the absorption bands recorded from thin surface films are expected to be independent of the angle of incidence and sensitive to the substrate orientation on the metal surface [17]. In the case of the pyridinium compound with

aliphatic chain (1-dodecylpyridinium chloride) used in this study, only vibrations non-parallel to the steel surface are expected to be detected in the infrared spectra.

For a rough surface, the polarization of the beam and the angle of incidence in relation to a particular surface facet cannot be established. A schematic presentation of the reverse Cassegrain optical path used in this study and applied in analysis of a topographically uneven (corrosion-roughened) steel surface is given in Fig. 2. The angle of incidence will vary due to the local topography of the surface and may be anywhere between 0º and 90º. Therefore, it is reasonable to assume that both polarizations of the beam, parallel (*p*) and perpendicular (*s*) are encountered in the course of the analysis (with multiple measurement points over a large surface area) and that there will be instances where a *p* or *s* component of the polarized beam relative to the surface facet is dominant.

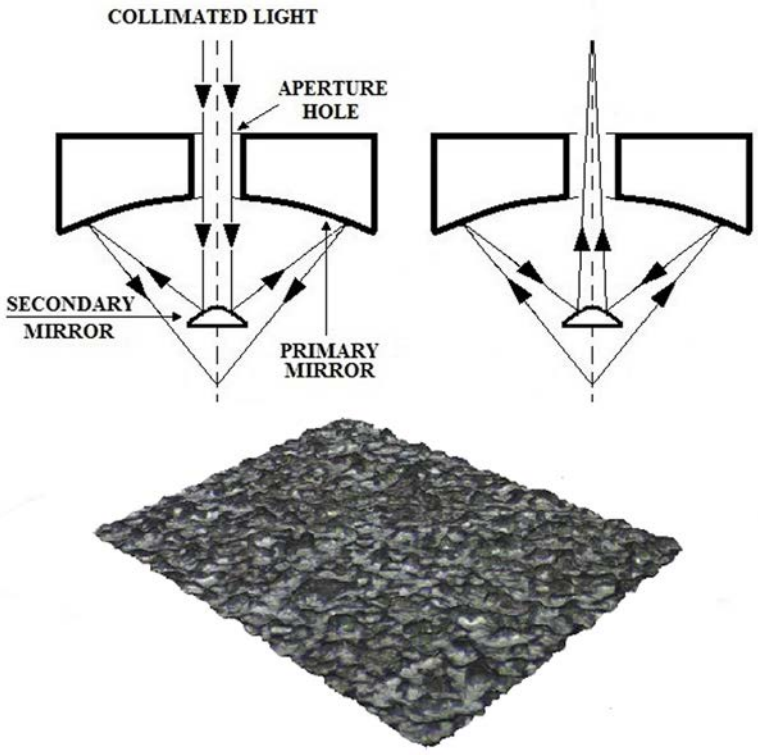

Fig. 2. Schematic presentation of reverse Cassegrain design objective used in analysis of topographically rough steel surface. The surface shown is a representative version of the highly complex corroded surface.

The formation of corrosion products at steel surface and the consequent increased roughness results in decreased reflectivity of the surface. Corroded metallic surfaces are at best semi-reflective and behave as semiconductors or non-conductors in terms of the reflection-absorption spectroscopy. At the semi-reflective and non-conductor surfaces, both *s* and *p*-polarizations have non-zero components in the electric field and vibrations in any direction (x, y, z) in respect to the surface can be detected. The optimal sensitivity of the absorption bands is observed at incidence angles of 60°-80° (*p*-polarization) and close to the surface normal (*s*-polarization). Furthermore, both positive and negative absorption bands can occur in the infrared spectra from a semiconductor or non-conductor, depending on the angle of the incidence beam with respect to the Brewster angle. With *p*-polarization, a maximum positive absorbance occurs just below the Brewster angle and maximum negative absorbance just above the Brewster angle. For *s*-polarization only negative absorbance occurs and is at a maximum at the normal angle of incidence. The presence of the positive or negative absorption bands in the spectra can provide information on the orientation of molecules in thin surface films [17].

3. RESULTS AND DISCUSSION

Atomic force microscopy (AFM) was used to investigate the adsorption of DPC at the steel surface. Fig. 3 shows images of the untreated (plain) steel (A) and DPC-treated steel (B) with a surface film of a well-defined structure. It should be noted that the roughness of the untreated

steel is approximately 0.45 µm. This may have implications for the infrared analysis as the surface roughness affects the local incidence angle of the infrared beam, as discussed previously.

The formation of the surface layer began immediately after immersion of the steel to the DPC-containing solution (1). The layer was fully formed after approximately 3 h exposure (shown in Fig. 3) and no further changes in its structure were observed. The AFM results clearly demonstrate that DPC adsorbs at the steel surface and that the surface film can be prepared by solution-deposition.

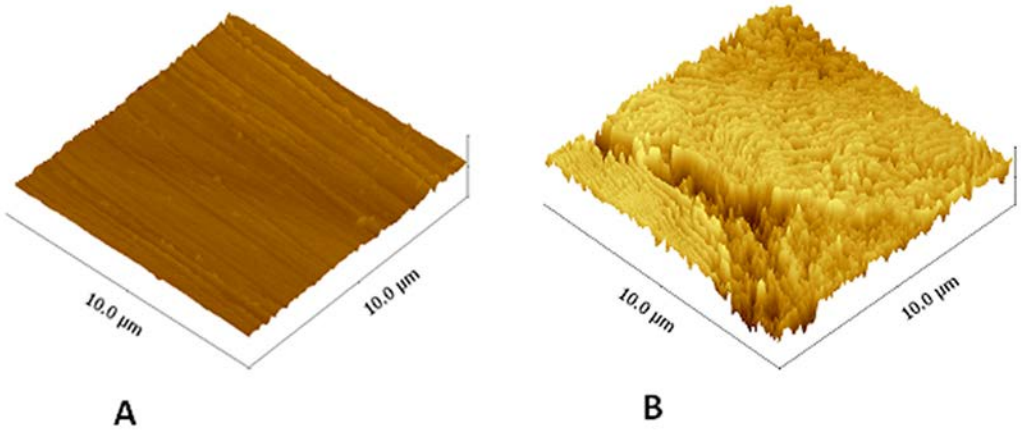

Fig. 3. AFM images of untreated (plain) steel (A) and DPC-deposited non-corroded steel (B).

The presence of DPC at the steel surface is further confirmed by linear polarization resistance analysis carried out in the presence and absence of the DPC in the corrosive testing solution (2). The respective corrosion rates measured in the presence and absence of DPC after 3 h exposure (consistent with the AFM data) were 1.9 and 4.9 mm y^{-1}, equivalent to 61% surface coverage with DPC. After 24 h immersion, the surface coverage increased to final value of 72%, calculated from the stabilized corrosion rates of 1.1 and 3.9 mm y^{-1}.

3.1 Infrared spectral analysis of DPC-deposited non-corroded steel

Fig. 4 shows infrared spectra from the untreated (plain) steel, bulk DPC powder and DPC-deposited non-corroded steel. Spectrum A is from the untreated steel and it is used as a background spectrum. It clearly shows that background contamination does not give rise to any spectral features. Spectrum B represents bulk powder of 1-dodecylpyridinium chloride hydrate (DPC). The absorption bands below 1650 cm^{-1} and in the region 3100-3010 cm^{-1} can be assigned to vibrations of the pyridinium ring and the aliphatic chain in the DPC molecule. The pyridinium ring C-H stretches occur between 3086 cm^{-1} and 3008 cm^{-1} and have medium intensity. The strong absorption bands at 2915 cm^{-1} and 2848 cm^{-1} represent C-H antisymmetric and symmetric stretching vibrations of the CH_2 groups of the aliphatic chain, respectively. The less intense absorption band at 2952 cm^{-1} is assigned to antisymmetric stretching of the CH_3 group of the aliphatic chain. The 3370 cm^{-1} band can be attributed to the O-H stretch of the water of crystallization of the hydrated form of DPC used [19]. A detailed assignment of the absorption bands of the DPC molecule below 1650 cm^{-1} is included in Table 1. Spectrum C is obtained from the DPC-deposited non-corroded steel. All the spectra obtained at more than 50 randomly selected measurement points at non-corroded steel and non-corroded areas of corroded samples were near identical in positions and relative intensities of the main absorption bands, suggesting that the micro-roughness of the surface did not influence these spectra. The most intense absorption bands are characteristic of CH_2 antisymmetric and symmetric stretching (2920 cm^{-1} and 2850 cm^{-1}) of the aliphatic chain of the DPC molecule. The CH_3 antisymmetric stretching (2954 cm^{-1}) is also evident. Much less intense absorption bands (inset in Fig. 4) were found below 1800 cm^{-1}. The band at 1466 cm^{-1} is attributed to aliphatic chain C-H deformation vibrations (antisymmetric) and/or -CH_2- scissor vibrations [19]. The absorption band at 1733 cm^{-1} was detected at non-corroded areas of corroded samples and is attributed to C=O stretching

vibrations of carbonic acid (H_2CO_3) and/or bicarbonate (HCO_3^-) [20] adsorbed at the steel surface treated in CO_2 media [21]. Overall, the absorption bands in spectrum C are attributed to the DPC molecule and confirm its presence at the steel surface. It is important to note that the C-H stretching vibrations of the pyridine ring in the DPC molecule, typically found in the wavelength region 3100-3000 cm^{-1}, were not observed in spectrum C from the DPC-deposited non-corroded steel. The C=C and C=N stretches of the ring at 1636 cm^{-1} and 1585 cm^{-1} were also not observed. As *s*-polarization has zero electric field intensity at a conductor surface, the positive absorbance bands observed in spectrum C are due to incident *p*-polarization radiation interacting with a molecule adsorbed on steel.

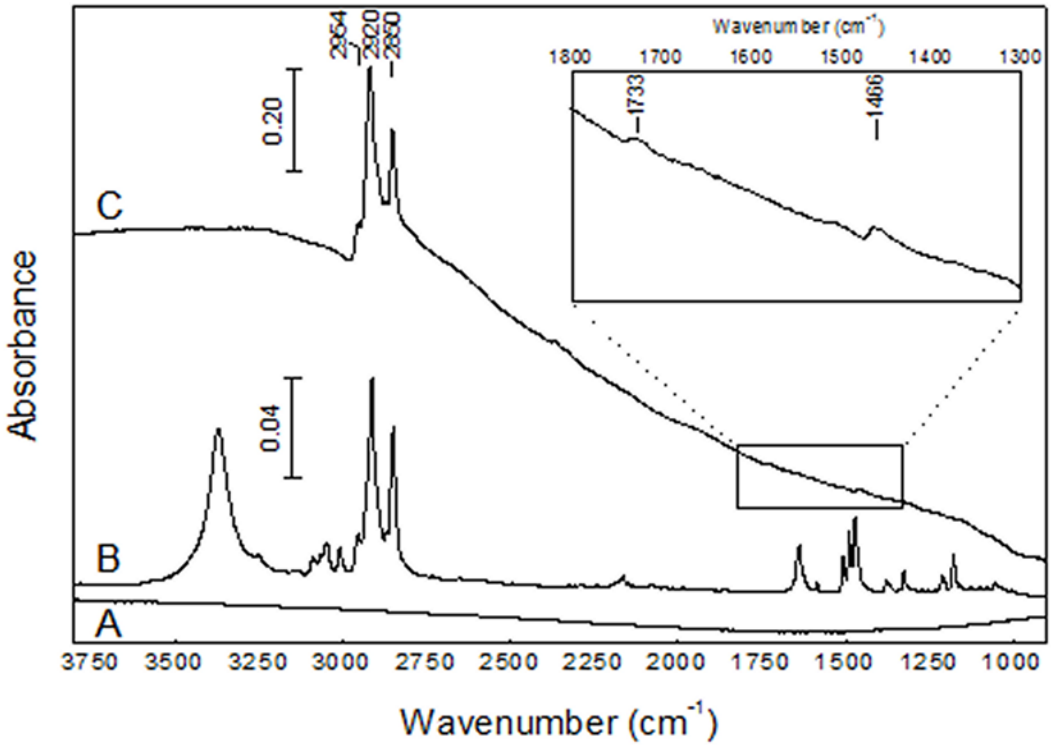

Fig. 4. Synchrotron infrared reflectance spectra of untreated steel (background spectrum, A), DPC powder (B) and DPC-deposited non-corroded steel (C). Band assignments are given in Table 1. Spectra are off-set for clarity.

It is worth noting that we have been unable to obtain meaningful spectra using a conventional (glow bar) infrared source and grazing angle accessory. Presumably because over to 25 x 50 mm area used in those attempts the samples are either too rough or not sufficiently flat, or both, or the source has insufficient intensity. These are not an issue with a 20 x 20 μm microscope aperture and ~8 μm synchrotron beam. A focal plane array FTIR microscope with aperture size of 100 x 100 μm and a conventional infrared source allowed detection of the absorption bands at the corroded steel surface. The spectral features obtained from these measurements were analogous to those shown in spectrum C in Figure 4 and confirmed the presence of DPC at the surface.

Table 1. Assignment of absorption bands shown in Fig. 4 from 1-dodecylpyridinium chloride hydrate (DPC) powder (spectrum B) and DPC-deposited non-corroded steel* (spectrum C) [19,20].

Wavenumber (cm^{-1})	**Band assignment**
1178, 1211	Pyridine ring C-H deformation vibrations (in-plane)
1325, 1377	Aliphatic chain C-H symmetric deformation vibrations
1466*	Aliphatic chain C-H antisymmetric deformation vibrations Aliphatic chain -CH_2- scissor vibration band
1471-1506	Pyridine ring stretching vibrations (C=C and C=N) Aliphatic chain -CH_2- scissor vibration band
1585, 1636	Pyridine ring stretching vibrations (in plane, C=C and C=N)
1733*	C=O stretching vibrations of carbonic acid (H_2CO_3) and/or bicarbonate ion (HCO_3^-)
2848 (2850*)	Aliphatic chain C-H symmetric stretching of CH_2 group
2915 (2920*)	Aliphatic chain C-H antisymmetric stretching of CH_2 group
2952 (2954*)	Aliphatic chain C-H antisymmetric stretching of CH_3 group
3008-3086	Pyridine ring C-H stretching vibrations
3370	O-H stretching, water of crystallization

3.1.1 Proposed orientation of DPC molecules at the steel surface

The spectrum of the DPC-deposited non-corroded substrate (Fig. 4C) was compared to that obtained from the bulk DPC compound (Fig. 4B) in order to determine the orientation of DPC at the steel surface. The absorption bands of the pyridinium ring would be expected in the regions below 1650 cm^{-1} and above 3010 cm^{-1}. However, the absorption bands detected in the region studied (3800-800 cm^{-1}) at the DPC-deposited steel surface are solely due to the aliphatic chain and out-of-plane C-H ring vibrations of the DPC molecule. The absence of absorption bands characteristic of in-plane vibrations of the pyridinium ring indicates that this part of the molecule is oriented flat (face-on/parallel) to the steel surface. In such an arrangement, the dipole transition moments of the aromatic C-H and pyridine ring stretches are parallel to the steel substrate, in which case no infrared absorption is observed.

The adsorption mechanism, resulting in a flat orientation of the pyridinium ring at the substrate, can be explained by π-electron interaction between the aromatic ring and the iron substrate and/or by π-electrostatic interaction of the negatively charged steel surface and positively charged pyridinium ion, that can be enhanced by halide ions pre-adsorbed at the substrate [10-12]. The proposed orientation of the aromatic ring of the DPC molecule at the steel substrate is consistent with literature published on the adsorption mechanism and orientation of pyridine and pyridinium compounds at modified metallic surfaces under similar conditions, mainly investigated with SERS [10-12,22].

The data in Fig. 4 also provides information on the orientation of the aliphatic chain of the DPC molecule in relation to the steel substrate. The presence and intensity of both the CH_2 symmetric and antisymmetric stretching vibrations in the spectra indicates that the aliphatic chain is tilted upwards from the steel substrate but is not perpendicular to it because a

perpendicular aliphatic chain (in relation to the substrate) would result in absorption by the antisymmetrical C-H stretching only [23]. The weak band at 1466 cm^{-1} (Fig. 4C) appears due to some parts of the chain giving a CH_2 deformation dipole change normal to the surface.

Additional information on the tilt angle between the aliphatic chain axis and the steel (and therefore the pyridinium ring oriented parallel to the substrate) can be derived from a comparison of the absorbance intensities of the aliphatic chain bands. A constant relative ratio of the absorption intensities of the aliphatic chain bands would imply a specific orientation of the aliphatic chain within the adsorbed layer relative to the steel surface [23,24]. In the current work, the ratio of the intensities of the CH_2 antisymmetric and symmetric vibrations were almost identical at all measurement points. The absorption bands and their relative intensities were also found to be almost identical to the spectra of the pure DPC compound (Fig. 4B). This suggests that there is a similar orientation of the aliphatic chain within the adsorbed layer on this microscopically rough surface as in DPC crystals. The crystallography of the pure DPC compound shows that the structure relationship between the planes of aromatic rings and the aliphatic chain is 79.16°, with a mean deviation of 0.005 Å [25]. This orientation of the chains is thus most likely to be the one that occurs in the DPC layer adsorbed at the steel substrate (Fig. 5).

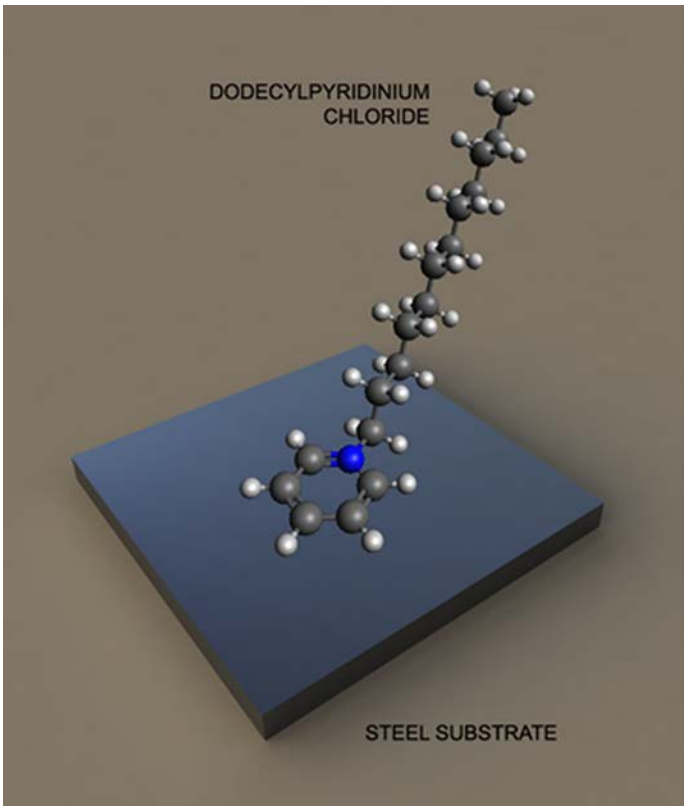

Fig. 5. Schematic presentation of the proposed orientation of the 1-dodecylpyridinium chloride molecule at the steel substrate.

3.2 Infrared spectral analysis of DPC-deposited corroded steel

Fig. 6 shows a microscope image of the DPC-deposited steel corroded in CO_2-saturated brine and the corresponding infrared spectra recorded at the analysis points indicated on the image. The surface is heterogeneous as a result of dissolution of the metal and/or the formation of the corrosion products, in addition to the DPC-deposition at the surface. More extensive corrosion appears at the darker area (surface inclusion) of the image (around measurement points 1-4) which is generally associated with high surface roughness. The roughness values (Rq) were approximately 0.53 µm at the less corroded areas and up to 1.28 µm at the more corroded areas (surface inclusions). The number, position and intensity ratios of the absorption bands from the

corroded steel are essentially identical to those recorded from the non-corroded steel (Fig. 4C). The absorption bands at 2954, 2920 and 2850 cm^{-1} (Fig. 6) are therefore again assigned to the DPC molecule at the steel surface. These results also suggest that the orientation of the DPC molecule at the surface is relatively unaffected by the degree of corrosion and that the proposed orientation, involving π-interaction between the pyridinium ring and the surface, applies to the DPC-deposited corroded steels.

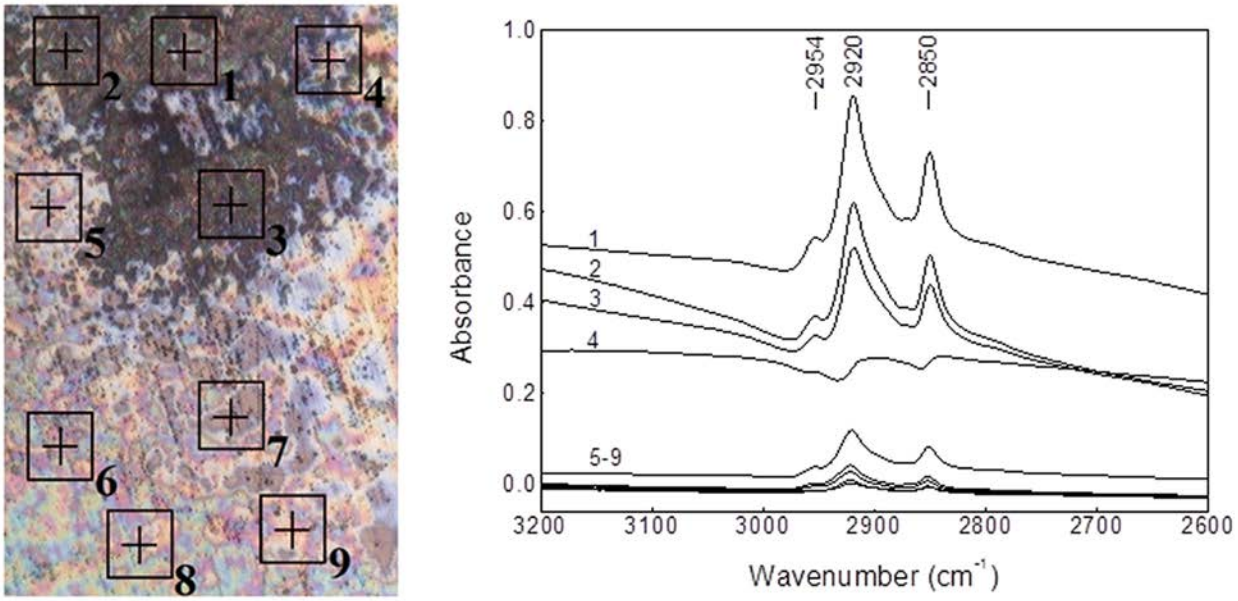

Fig. 6. Microscope image of DPC-deposited corroded steel with marked analysis points (20 x 20 μm) and the corresponding infrared reflectance spectra. Spectra are shown as recorded.

The data in Fig. 6 show that the amount of adsorbed DPC varies across the studied surface. The higher absorbances recorded at the more corroded analysis areas (1-4) are indicative of a greater DPC adsorption than that which occurs on the less corroded analysis area (5-9). The greater DPC adsorption can be associated with the higher surface roughness and/or the preferable adsorption of DPC to corrosion products at the more corroded areas. The formation of iron oxide/hydroxide/carbonate species can be expected in carbon dioxide media [26,27] but in this

study no absorption bands characteristic of corrosion products are evident in the spectra in Fig. 6 nor observed in the 1800-800 cm^{-1} region. More interestingly, one of the spectra (4) in Fig. 6 showed negative absorbance bands.

Polarization of the infrared beam and its angle of incidence with respect to the Brewster angle define whether positive or negative spectra are observed. The effect of surface topography and reflectivity on the appearance of the positive or negative absorption bands is further demonstrated in Fig. 7, which shows the grid map of analysis points of a larger area of the DPC-deposited corroded steel compared to that in Fig. 6. It was found that positive spectra (analysis points 1, 4 and 6) are recorded across almost the entire surface irrespective of the degree of corrosion, whereas the negative spectra (analysis points 2, 3 and 5) are specific to the more corroded areas (surface inclusions) or their close proximity. The appearance of both the positive and negative spectra at the more corroded areas can be explained by a combined effect of having both conductor (steel) and non-conductor (corrosion products) and a wider variation in the local angle of incidence as a function of increased roughness. The positive bands arise from the interaction of the *p*-polarized radiation with DPC adsorbed at a steel (conducting surface). The negative bands arise from the interaction of *p*-polarized radiation at angles greater than the Brewster angle, or *s*-polarized radiation, with DPC adsorbed on corrosion products (non-conducting). As we did not observe any in-plane C-H stretches nor in-plane pyridine ring vibrations it suggests that the negative bands arise from *p*-polarized radiation.

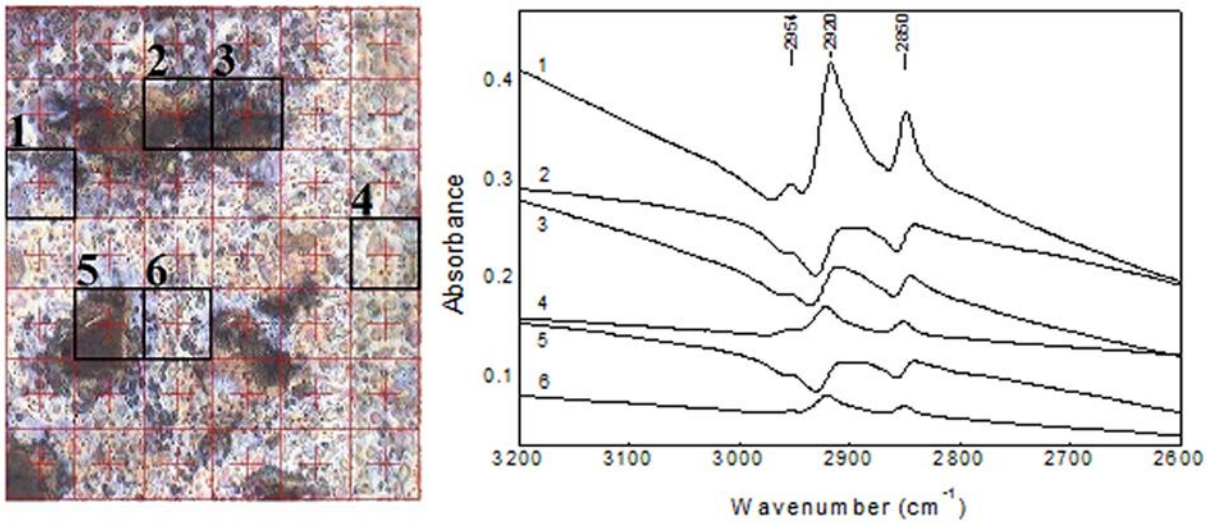

Fig. 7. Microscope image of DPC-deposited corroded steel with marked analysis points (20 x 20 μm) and the corresponding infrared reflectance spectra, positive (1, 4, 6) and negative (2, 3, 5). Spectra are off-set for clarity.

The observation of negative and positive infrared bands for corroded steel surfaces is analogous to variable angle polarized infrared beam measurements with a plane surface. In this instance it definitively confirms the π-bonded adsorption orientation of DPC on steel indicated by the non-corroded surface data. This orientation most probably also occurs on the corrosion products.

4. CONCLUSIONS

Synchrotron infrared microspectroscopy has been applied to study the adsorption of 1-dodecylpyridinium chloride (DPC) on non-corroded mild steel and mild steel corroded in carbon dioxide media. These complex surfaces represent real-life systems and are used to demonstrate the applicability of the infrared method to the analysis of organic film at a microscopically rough

metal surface. Infrared spectra, analogous to polarized grazing angle spectra at varying angles of incidence were recorded. Positive and negative absorption intensities are observed at different measurement locations. These intensity changes are interpreted in terms of optical effects, their variation due to the uneven topography of the surface and a change from conductor to non-conductor substrates.

The presence of DPC at the steel surface is confirmed by the C-H stretching vibrations of the CH_2 and CH_3 groups of the aliphatic chain in the infrared spectra. The proposed surface orientation of DPC is derived from the presence and absence of absorption bands characteristic of the aliphatic chain and pyridinium ring, respectively, in the infrared spectra. The pyridinium ring of the DPC molecule is oriented flat at the surface and its aliphatic chain is tilted upwards from the substrate at ~79°, i.e. not perpendicular to it. The DPC adsorption mechanism proposed involves π-electron interaction between the aromatic ring and the steel substrate.

ACKNOWLEDGMENT

This research was undertaken on the Infrared microspectroscopy beamline at the Australian Synchrotron, Clayton, Australia. The assistance of Dr. Mark Tobin and Dr. Danielle Martin is greatly acknowledged. The authors thank Curtin University for a Curtin Research Fellowship (K.L.) and a Curtin International Postgraduate Research Scholarship (V. P.).

REFERENCES

[1] R. Atkin, V.S.J. Craig, E.J. Wanless, S. Biggs, Adv. Colloid Interface Sci. 103 (3) (2003) 219-304.

[2] C.C. Nathan, Corrosion Inhibitors, National Association of Corrosion Engineers, Houston, TX, 1981.

[3] W. Durnie, R. de Marco, A. Jefferson, B. Kinsella, J. Electrochem. Soc. 146 (5) (1999) 1751-1756.

[4] S.A. Francis, A.H. Ellison, J. Opt. Soc. Am. 49 (2) (1959) 131-138.

[5] R.G. Greenler, J. Chem. Phys. 44 (1) (1966) 310-315.

[6] P.R. Griffiths, J.A. de Haseth, Fourier Transform Infrared Spectrometry. Chemical Analysis, Vol. 83, J. Wiley & Sons, NY, 1986.

[7] A. Frigani, F. Zucchi, C. Monticelli, Br. Corros. J. 18 (1) (1983) 19-24.

[8] C.C. Nathan, in: C.C. Nathan (Ed.), Corrosion Inhibitors, National Association of Corrosion Engineers, Houston, TX, 1981, pp. 42-54.

[9] H. Yamada, Y. Yamamoto, Surf. Sci. 134 (1) (1983) 71-90.

[10] K. Aramaki, J. Uehara, J. Electrochem. Soc. 136 (5) (1989) 1299-1303.

[11] K. Aramaki, M. Ohi, J. Uehara, J. Electrochem. Soc. 139 (6) (1992) 1525-1529.

[12] J. Uehara, H. Nishihara, K. Aramaki, J. Electrochem. Soc. 137 (9) (1990) 2677-2683.

[13] ASTM G102-89, Standard Practice for Calculation of Corrosion Rates and Related Information from Electrochemical Measurements, ASTM International, 2010.

[14] G. Santoro, I. Yousef, F. Jamme, P. Dumas, G. Ellis, Rev. Sci. Instrum. 82 (2011) 033710.

[15] G. Ellis, M.A. Gomez, C. Marco, J. Macromol. Sci., Phys. 43 (1) (2005) 191-206.

[16] G. Ellis, C. Marco, M. Gomez, Infrared Phys. Technol. 45 (2004) 349-364.

[17] J.A. Mielczarski, J. Phys. Chem. 97 (11) (1993) 2649-2663.

[18] G.T. Merklin, P.R. Griffiths, J. Phys. Chem. B 101 (1997) 7408-7413.

[19] G. Socrates, Infrared Characteristic Group Frequencies. Tables and Charts, 2nd edn., J. Wiley & Sons, Chichester, 1994.

[20] W. Hage, A. Hallbrucker, E. Mayer, J. Am. Chem. Soc. 115 (1993) 8427.

[21] A. Wieckowski, E. Ghali, M. Szklarczyk, J. Sobkowski, Electrochim. Acta 28 (1983) 1619.

[22] W. Durnie, R. de Marco, A. Jefferson, B. Kinsella, J. Surf. Interface Anal. 35 (6) (2003) 536-543.

[23] G.A. Salensky, M.G. Cobb, E.S. Everhart, Ind. Eng. Chem. Prod. Res. Dev. 25 (2) (1986) 133-140.

[24] W.G. Golden, C.D. Snyder, B. Smith, J. Phys. Chem. 86 (24) (1982) 4675-4678.

[25] K. Vongbupnimit, K. Noguchi, K. Okuyama, Acta Crystallogr. C51 (1995) 1940-1941.

[26] M.B. Kermani, A. Moshed, Corrosion. 59 (8) (2003) 659-683.

[27] R. de Marco, Z.-T. Jiang, B. Pejcic, E. Poinen, J. Electrochem. Soc. 152 (10) (2005) B389-B392.